

Monte Carlo calculation of the surface tension for two- and three-dimensional lattice-gas models

K. Binder

*Institut für Festkörperforschung, Kernforschungsanlage Jülich,
Postfach 1913, D-5170 Jülich, West Germany*

(Received 18 August 1981)

It is suggested that the interface free energy between bulk phases with a macroscopically flat interface can be estimated from the variation of certain probability distribution functions of finite blocks with block size. For a liquid-gas system the probability distribution of the density would have to be used. The method is particularly suitable for the critical region where other methods are hard to apply. As a test case, the two-dimensional lattice-gas model is treated and it is shown that already, from rather small blocks, one obtains results consistent with the exact solution of Onsager for the surface tension, by performing appropriate extrapolations. The surface tension of the three-dimensional lattice-gas model is also estimated and found to be reasonably consistent with the expected critical behavior. The universal amplitude of the surface tension of fluids near their critical point is estimated and shown to be in significantly better agreement with experimental data than the results of Fisk and Widom and the first-order $4-d$ renormalization-group expansion. Also the universal amplitude ratio used in nucleation theory near the critical point is estimated.

I. INTRODUCTION

The traditional way of calculating the "surface tension" F_s associated with the interface between coexisting phases has been based on the profile $\rho(x)$ of the order parameter ρ distinguishing the phases in the direction x across the interface.²⁻¹⁰ As has been beautifully reviewed by Widom,¹¹ there still exist severe conceptual difficulties with this approach: (i) The appropriate choice of free-energy density for values of the order parameter in between the values occurring in the bulk of the coexisting phases has been doubtful, particularly in the critical region where fluctuation effects are important. (ii) For systems of dimensionality $d = 3$ or less, there exists a long-wavelength interface instability due to capillary waves.^{12,13} In the absence of fields stabilizing the position of the interface, such as the gravitational field which stabilizes the liquid-gas interface, the profile $\rho(x)$ is not well defined in the thermodynamic limit. The width of the interface $w_d(L)$ in a D -dimensional system with linear dimension(s) L parallel to the interface [Fig. 1(a)] diverges for $L \rightarrow \infty$ as $w_d(L) \propto L^{(3-d)/2}$ [or $\propto (\ln L)^{1/2}$ for $d = 3$]. Although due to this instability $\rho(x)$ is not well defined, there exists a well-defined interface free energy. For example, this instability also occurs in the two-dimensional lattice gas model¹³ where the interface free energy has been calculated exactly.¹⁴

While the first difficulty, the choice of the free-energy functional, is remedied in the critical region by a renormalization-group approach,¹⁰ at least to the extent that an expansion in $\epsilon = 4 - d$ is accurate for $d = 3$, it is not clear whether in this approach a meaningful treatment of the capillary wave instability is possible, since it does not occur at all for $d > 3$.¹⁵

Most numerical calculations of the interface free energy using computer simulations have also been based on the use of $\rho(x)$ in the context of suitable generalizations of van der Waals theory.¹⁶ Since one is treating rather small systems, fluctuations which correspond to long-wavelength capillary waves cannot even occur. One then also may use periodic boundary conditions in the direction parallel to the interface [Fig. 1(b)]. A recourse to van der Waals-type theories can be avoided by comparing a system containing an interface [Fig. 1(b)] to another system without an interface, but otherwise identical conditions.¹⁷ This can be done by choosing boundary conditions as indicated in Fig. 1(c). Studying the excess energy U_s of the system of Fig. 1(b) in comparison with that of Fig. 1(c), one can find that interface free energy F_s by numerical integration,

$$F_s/k_B T = \int d \left[\frac{1}{k_B T} \right] U_s .$$

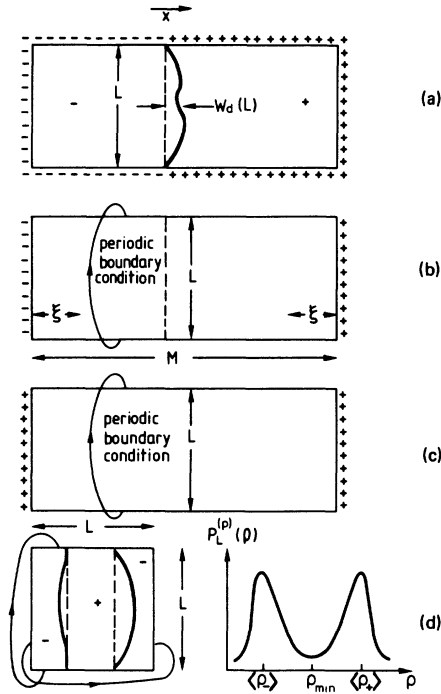


FIG. 1. (a) Boundary conditions for a two-dimensional Ising system which lead to the formation of an interface below the critical point: spins are fixed at ± 1 as indicated at the boundaries. Thick solid line denotes the (coarse-grained) position of the interface between the phases with negative and positive magnetization in a typical spin configuration. (b) Standard boundary conditions for the computer simulation of a system containing an interface. Note that the linear dimensions $M \gg 2\xi$, where ξ is the bulk correlation length of order-parameter fluctuations. (c) Boundary for a reference system without an interface. (d) Finite system with all boundary conditions periodic and its order-parameter distribution function $P_L^{(p)}(\rho)$. The minimum of $P_L^{(p)}(\rho)$ corresponds to a situation with two interfaces, while the maxima correspond to pure phases with order parameters $\langle \rho_- \rangle$ and $\langle \rho_+ \rangle$, respectively.

If the linear dimensions L, M are both much larger than the correlation length ξ of the order-parameter fluctuations, one would include possible capillary wave fluctuation contributions to the interface free energy by this method.

While this method clearly is useful for temperatures far below critical, and there it has also been generalized to Lennard-Jones fluids,¹⁸ it is cumbersome to apply near the critical point: There ξ is very large, the U_s becomes very small. At the same time, the fluctuations of the bulk energy of order $(ML^{d-1}C_T)^{1/2}$ strongly increase, because the bulk specific heat C_T would diverge in the

thermodynamic limit at the critical point. Hence it is difficult to obtain the excess energy (of order $L^{d-1}U_s$) very accurately.¹⁷

In the present paper we are concerned with a new method for obtaining the interface free energy in the critical region. We exploit the observation¹⁹ that near T_c there is an observable probability that interfaces form *spontaneously in a finite system* due to thermal fluctuations, since the interface free energy is so small. The order-parameter probability distribution $P_L^{(p)}(\rho)$ has a *nonzero* minimum value $P_L^{(p)}(\rho_{\min})$ for a state with two interfaces [Fig. 1(c)].²⁰ Here the index (p) stands for periodic boundary conditions. From the variation of $P_L^{(p)}(\rho_{\min})$ with linear dimension L the interface free energy is extracted. Since there are no fixed-spin boundary conditions in this method, the interface positions are not pinned (apart from interface pinning due to the finiteness of L , which effects are eliminated by suitable extrapolation to $L \rightarrow \infty$).

In Sec. II this method is explained in more detail. Also the related problem is discussed where one studies $P_L(\rho_{\min})$ for blocks of volume L^d which are the subsystem of a much larger system.¹⁹ Section III shows that for the two-dimensional lattice gas relatively small lattice sizes yield estimates for the surface tension consistent with the exact solution. In Sec. IV this method is applied to the three-dimensional lattice gas, and it is shown that the estimated surface tension is consistent with the expected critical behavior. In Sec. V the estimated critical amplitude of the surface tension is used to calculate the universal amplitude ratio $\beta^2 c$ associated with the surface tension. It is shown that our estimate for $\beta^2 c$ is in somewhat better agreement with corresponding experimental data for real fluids than the theory of Fisk and Widom⁵ or first-order ϵ -expansion results ($\epsilon = 4 - d$).¹⁰ Section VI summarizes our conclusions.

II. ORDER-PARAMETER BLOCK DISTRIBUTION FUNCTIONS AND DOMAIN CONFIGURATIONS

We consider a finite system of volume L^d with periodic boundary conditions at a temperature below the critical temperature T_c , where a phase separation into phases with order parameters $\langle \rho_- \rangle$, $\langle \rho_+ \rangle$ occurs. In a liquid-gas system, the order parameter is the density, $\langle \rho_- \rangle$ is the gas density, and $\langle \rho_+ \rangle$ the liquid density; in a binary mixture AB with a miscibility gap, $\langle \rho_- \rangle$ and $\langle \rho_+ \rangle$ are the relative concentrations $c_{B,1}^{(\text{coex})}$, $c_{B,2}^{(\text{coex})}$

of the coexisting A -rich and B -rich phases; in an Ising magnet, $\langle \rho_- \rangle$ and $\langle \rho_+ \rangle$ correspond to the two orientations $\pm M$ of the spontaneous magnetization M . The chemical potential μ of the liquid-gas system (or the chemical potential difference $\Delta\mu$ between A and B species in the case of the mixture, or the magnetic field H in the case of the Ising magnet) has to be fixed at precisely that value that would correspond to coexisting phases in the thermodynamic limit.

If we were to consider fluctuations in a pure phase, the probability distribution would be a Gaussian, for $L \rightarrow \infty$,

$$P_L^{(p)}(\rho) = L^{d/2} (2\pi k_B T \chi)^{-1/2} \times \exp[-(\rho - \langle \rho \rangle)^2 L^d / (2k_B T \chi)], \quad (1)$$

χ being the order-parameter ‘‘susceptibility’’ ($\chi = (\partial\rho/\partial\mu)_T$ for the liquid-gas system, $\chi = [\partial c_B/\partial(\Delta\mu)]_T$ for the binary mixture, and $\chi = (\partial M/\partial H)_T$ for the Ising magnet, respectively). Neglecting configurations which contain domains describing states with mixed phases, a state at the coexistence curve when both coexisting phases are equally likely to occur, would then have the probability distribution

$$P_L^{(p)}(\rho) \cong \frac{1}{2} L^{d/2} (2\pi k_B T \chi_-)^{-1/2} \exp[-(\rho - \langle \rho_- \rangle)^2 L^d / (2k_B T \chi_-)] + \frac{1}{2} L^{d/2} (2\pi k_B T \chi_+)^{-1/2} \exp[-(\rho - \langle \rho_+ \rangle)^2 L^d / (2k_B T \chi_+)], \quad (2)$$

where χ_- , χ_+ are the values of the susceptibility at the two branches of the coexistence curve. According to Eq. (2), a state with order parameter $\rho_{\min} = (\langle \rho_- \rangle + \langle \rho_+ \rangle)/2$ would have a probability of order

$$L^{d/2} (2\pi k_B T \chi)^{-1/2} \exp[-(\langle \rho_+ \rangle - \langle \rho_- \rangle)^2 L^d / (2k_B T \chi)];$$

i.e., the probability of a *homogeneous* state with order parameter ρ_{\min} decreases exponentially fast with the volume L^d of the system. Hence for large enough L , ‘‘homophase fluctuations’’ with $\rho = \rho_{\min}$ will have negligible weight in comparison with ‘‘heterophase fluctuations’’, whose probability decreases exponentially fast with the interface area $2L^{d-1}$ (Refs. 19 and 21),

$$P_L^{(p)}(\rho_{\min}) \propto P_L^{(p)}(\langle \rho_+ \rangle) \exp(-2L^{d-1} F_s / k_B T). \quad (3)$$

The size dependence of the preexponential factor

$$P_L^{(p)}(\langle \rho_+ \rangle) \cong \frac{1}{2} L^{d/2} (2\pi k_B T \chi_+)^{-1/2}$$

is much weaker than the exponential variation. In fact, we do expect other preexponential factors which may also vary with L according to power laws, and hence may be of the same order of magnitude as $P_L^{(p)}(\langle \rho_+ \rangle)$.

(i) Since the free energy associated with a domain configuration such as shown in Fig. 1(d) is invariant against a translation of the domain, the phase space associated with these ‘‘Goldstone modes’’ will lead to an additional preexponential factor.

(ii) Interface shapes other than planar [such as indicated in Fig. 1(d)] for large L are yielding negligible contributions only if the deviation from planar interfaces is large; small deviations are

nothing else but capillary waves which we wish to include in F_s , if they make a contribution there at all. These capillary waves are expected to contribute to the preexponential factor as well. At the same time, capillary waves with wavelengths other than $2L/n$, $n = 1, 2, \dots$, are excluded due to the periodic boundary condition. As a result, F_s in Eq. (3) can be considered as having L -dependent corrections. Formally these corrections can also be included into the L -dependent preexponential proportionality factor.

As a result, a theory for the L dependence of the preexponential factor in Eq. (3) seems rather difficult and is not attempted here. In any case, it is plausible from the above discussion that the asymptotic form of $P_L^{(p)}(\rho_{\min})$ for large L should be

$$P_L^{(p)}(\rho_{\min}) = A L^x \exp(2L^{d-1} F_s / k_B T), \quad (4)$$

where neither the exponent x nor the constant A is known. But $F_s / k_B T$ can then be extracted from $P_L^{(p)}(\rho_{\min})$ considering the limiting processes

$$\begin{aligned} \frac{F_s}{k_B T} &= \lim_{L \rightarrow \infty} \frac{F_L^{(1)}}{k_B T} \\ &= \lim_{L \rightarrow \infty} \frac{1}{2L^{d-1}} \ln \left[\frac{P_L^{(p)}(\langle \rho_+ \rangle)}{P_L^{(p)}(\rho_{\min})} \right], \end{aligned} \quad (5a)$$

or

$$\frac{F_s}{k_B T} = \lim_{L \rightarrow \infty} \frac{F_L^{(2)}}{k_B T} = \lim_{L \rightarrow \infty} \frac{1}{2L^{d-1}} \ln P^{(\rho)}(\rho_{\min}) . \quad (5b)$$

In a numerical method, where these limits cannot be carried through analytically, one has to estimate $F_s/k_B T$ by a suitable numerical extrapolation.

Three procedures are conceivable. (i) fitting a straight line to a plot of $\ln P_l^{(\rho)}(\rho_{\min})$ vs. L^{d-1} ; (ii) Since Eqs. (4) and (5) imply that (A' being another constant)

$$\frac{F_l^{(2)}}{k_B T} = \frac{F_s}{k_B T} - \frac{x \ln L}{2L^{d-1}} - \frac{\ln A}{2L^{d-1}} , \quad (6a)$$

$$\frac{F_l^{(1)}}{k_B T} = \frac{f_s}{k_B T} - \frac{(x-d/2)\ln L}{2L^{d-1}} - \frac{\ln A'}{2L^{d-1}} , \quad (6b)$$

one can extrapolate $F_l^{(1)}/k_B T$, $F_l^{(2)}/k_B T$ linear in the variable $\ln L/L^{d-1}$, assuming that x (and $x-d/2$) are nonzero. (iii) For small L , however, it may happen that $x \ln L < \ln A$ [or $(x-d/2) \ln L < \ln A'$], and then an extrapolation linear in the variable $1/L^{d-1}$ is more appropriate. This point has to be checked with the numerical data available (see below).

One can also consider the related problem of studying the order-parameter distribution $P_L(\rho)$ for a system of size L^d being the subsystem of a much larger system.¹⁹ Then $P_L(\rho_{\min})$ will for large L be dominated by a configuration of a compact domain of size $\frac{1}{2}L^d$, the shape of this domain being given by the condition that the total interface free energy is a minimum. For continuum systems, as well as for Ising systems near their critical points, the surface tension should not depend on the interface orientation, and hence the total interface free energy is a minimum for a (hyper) spherical domain shape. As a result, one should have, apart from preexponential factors,

$$P_L(\rho_{\min}) \propto \exp[-S_d(2V_d)^{-(d-1)/d} L^{d-1} F_s/k_B T] , \quad (7)$$

where S_d and V_d are the surface area and volume of a d -dimensional unit sphere. For (cubic) Ising systems outside the critical region, the surface tension does depend on the interface orientation, and hence the domain shape is no longer spherical, irrespective of the size of the domain.^{22,23} Then one no longer is able to extract the surface tension itself from $P_L(\rho_{\min})$, but one still gets the total interface free energy of a domain of volume $L^{d/2}$. For $T \rightarrow 0$ the shape of the domain is expected to be-

come a square^{22,23} or (hyper) cube, respectively; in this limit again the surface tension of planar interfaces enters, the contribution due to edges and corners being negligible. Hence

$$P_L(\rho_{\min}) \propto \exp(-d 2^{1/d} L^{d-1} F_s/k_B T), \quad T \rightarrow 0 . \quad (8)$$

This fact suggests defining an enhancement factor $\epsilon(T) \equiv F_s^{\text{eff}}/F_s$ by defining F_s^{eff} from using Eq. (7) at all temperatures,

$$P_L(\rho_{\min}) \propto \exp[-S_d(2V_d)^{-(d-1)/d} L^{d-1} F_s^{\text{eff}}/k_B T] . \quad (9)$$

In lattice systems $\epsilon(T)$ varies between unity (at T_c) and

$$\epsilon(0) = 2d^{1/d} (2V_d)^{(d-1)/d} / S_d .$$

For $d=2$,

$$\epsilon(0) = 2/\sqrt{\pi} \approx 1.13 ;$$

for $d=3$,

$$\epsilon(0) = 2 \left[\frac{3}{4\pi} \right]^{1/3} \approx 1.24 .$$

III. TWO-DIMENSIONAL ISING MODEL

In order to test the methods outlined in Sec. II, we have performed Monte Carlo calculations for two-dimensional Ising square lattices, where a comparison is possible with the exact surface tension of a planar interface parallel (100) direction,¹⁴

$$F_s = 2J - k_B T \ln[(1 + e^{-2J/k_B T})/(1 - e^{-2J/k_B T})] , \quad (10)$$

where J is the nearest-neighbor exchange (Hamiltonian $\mathcal{H} = -J \sum S_i S_j$, $S_i = \pm 1$). Lattice sizes L chosen have been $L=2-10, 12, 15, 16, 20$, with periodic boundary conditions; in the case of subsystem blocks, a lattice was chosen with linear dimension $N=60$ and periodic boundaries, which thus enabled us to use $L=2-6, 10, 12, 15, 20$.²⁴ In the Ising system, the order parameter ρ is usually related to the magnetization $s = (1/L^d) \sum S_i$ of the lattice, and due to the symmetry of this model the order parameter satisfies a symmetry relation

$$\langle S_- \rangle = 1 - 2 \langle \rho_- \rangle = - \langle S_+ \rangle = - (1 - 2 \langle \rho_+ \rangle) ,$$

and hence ρ_{\min} corresponds to $s=0$.

Figure 2 shows data obtained for both $P_L^{(p)}(s=0)$ and $P_L(s=0)$, for temperatures between T_c and about $0.8 T_c$. The straight lines seen in Fig. 2 indicate that the data are consistent with the expected exponential decay, Eqs. (3) and (7). Since these probabilities quickly become very small with increasing linear dimension, it is clear that it would be very hard to obtain data of meaningful accuracy at either lower temperatures and/or larger sizes than studied. As expected, however, data for very small L do not fit to a straight-line behavior in the semilogarithm-plots of Fig. 2 yet, and hence one has to be rather careful in using these data to estimate F_s . This is obvious from Fig. 3, where the estimates for $F_s/k_B T$ which would follow from the slopes shown in Fig. 2 are compared to Eq. (10). Although the general trend with temperature is given correctly, in particular it is seen that $F_s/k_B T$ vanishes at the critical temperature [$k_B T_c/J$

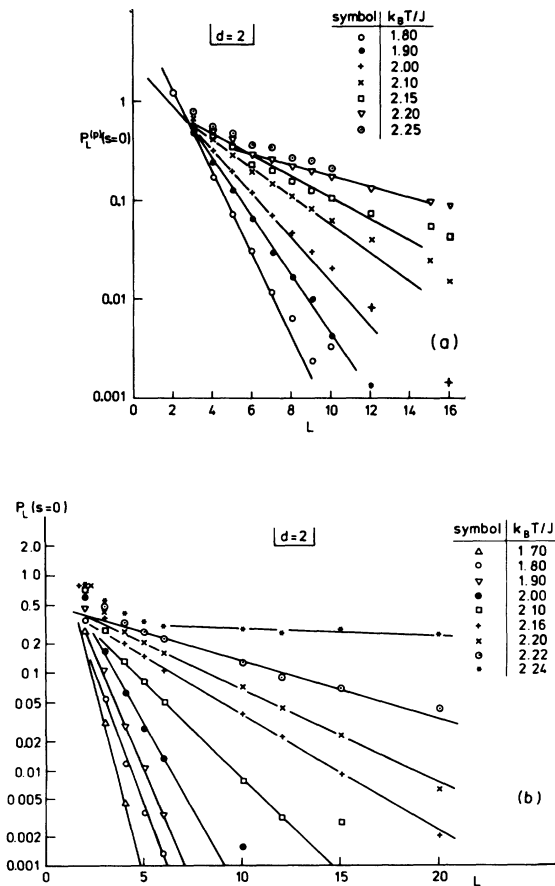


FIG. 2. Semilogarithm plot of $P_L^{(p)}(0)$ vs L (a) and $P_L(0)$ vs L (b), for the nearest-neighbor two-dimensional square Ising model and a variety of temperatures.

≈ 2.269 (Ref. 14)], and it is seen that data obtained from $P_L^{(p)}(s=0)$ and $P_L(s=0)$ do not agree with each other, and lie systematically above the correct values given by Eq. (10).

We thus attempt to use Eq. (6). Figure 4 shows that a linear extrapolation of both $\ln P_L^{(p)}(0)/L$ and $\ln[P_L^{(p)}(s_{\max})/P_L^{(p)}(0)]$ vs $1/L$ yields results consistent with each other, and with the exact result, Eq. (10). The particularly pronounced linearity of the data for $\ln P_L^{(p)}(0)/L$ suggests that the (effective) exponent x in Eq. (6) must be near zero for $d=2$. The data for $\ln P_L(0)/L$, on the other hand, would not yield the correct result if one tried to extrapolate them linearly in $1/L$, too. Here the geometric factor of Eq. (7), appropriate for spherical domains, rather than that of Eq. (8), appropriate for square-shaped domains, is used. Even using the latter would not remedy this discrepancy. In addition, the deviations from spherical domain shape close to T_c are expected to be negligible.^{22,23} We attribute this discrepancy to the fact that a different value of the exponent x applies for $P_L^{(p)}(s=0)$ and $P_L(s=0)$, with the exponent x appropriate for $P_L(s=0)$ not being close to zero. In fact, Fig. 5 shows that while an extrapolation of $\ln P_L^{(p)}(s=0)/L$ (or $\ln[P_L^{(p)}(s_{\max})/P_L^{(p)}(0)]/L$, respectively) vs the variable $\ln L/L$ tends to underestimate the correct results (if one uses an extrapolation as indicated by the dash-dotted lines), the data for $\ln P_L(s=0)/L$ now seem consistent with the exact result. Of course, it is natural to assume

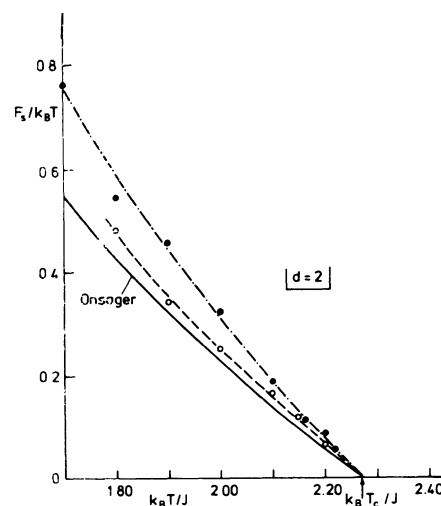


FIG. 3. Preliminary estimates of $F_s/k_B T$ for the two-dimensional Ising model, using the slopes indicated in Fig. 2(a) (open circles) and Fig. 2(b) (full circles). Full curve represents Eq. (10).

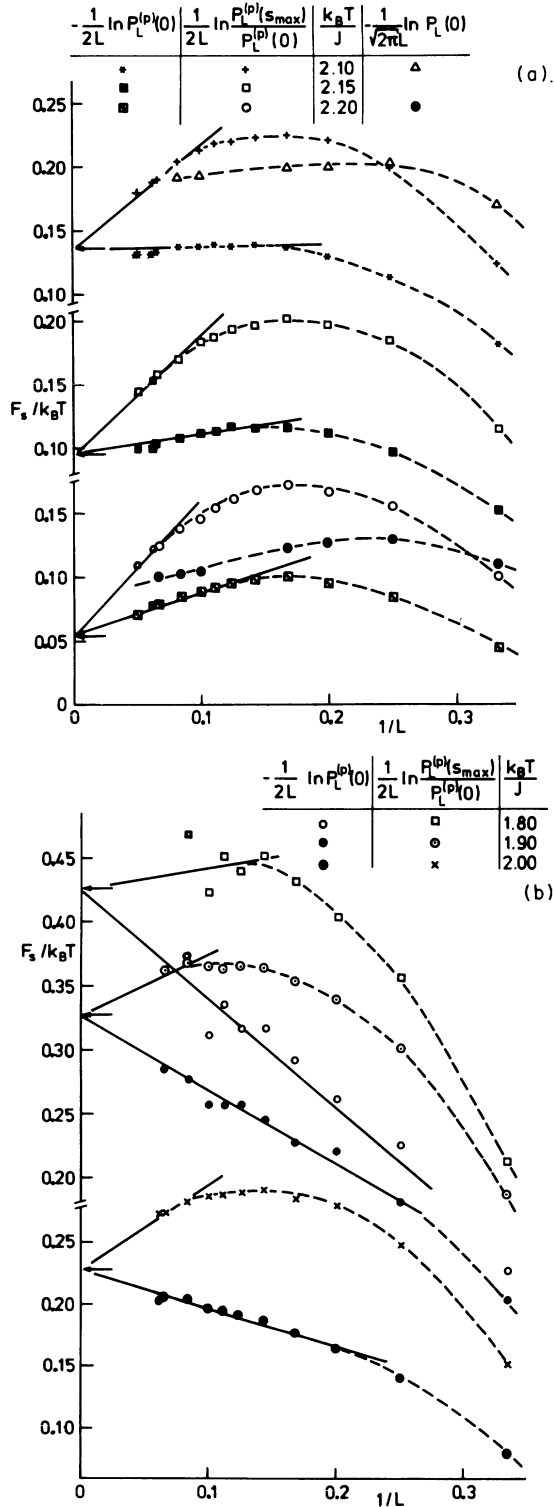


FIG. 4. Extrapolation of $\ln P_L^{(p)}(0)/L$ and $\ln[P_L^{(p)}(s_{\max})/P_L^{(p)}(0)]/L$ vs $1/L$, for three temperatures close to T_c (a) and further below T_c (b), for the two-dimensional Ising model. Some data for $\ln P_L(0)/L$ are also included. Arrows indicate Eq. (10).

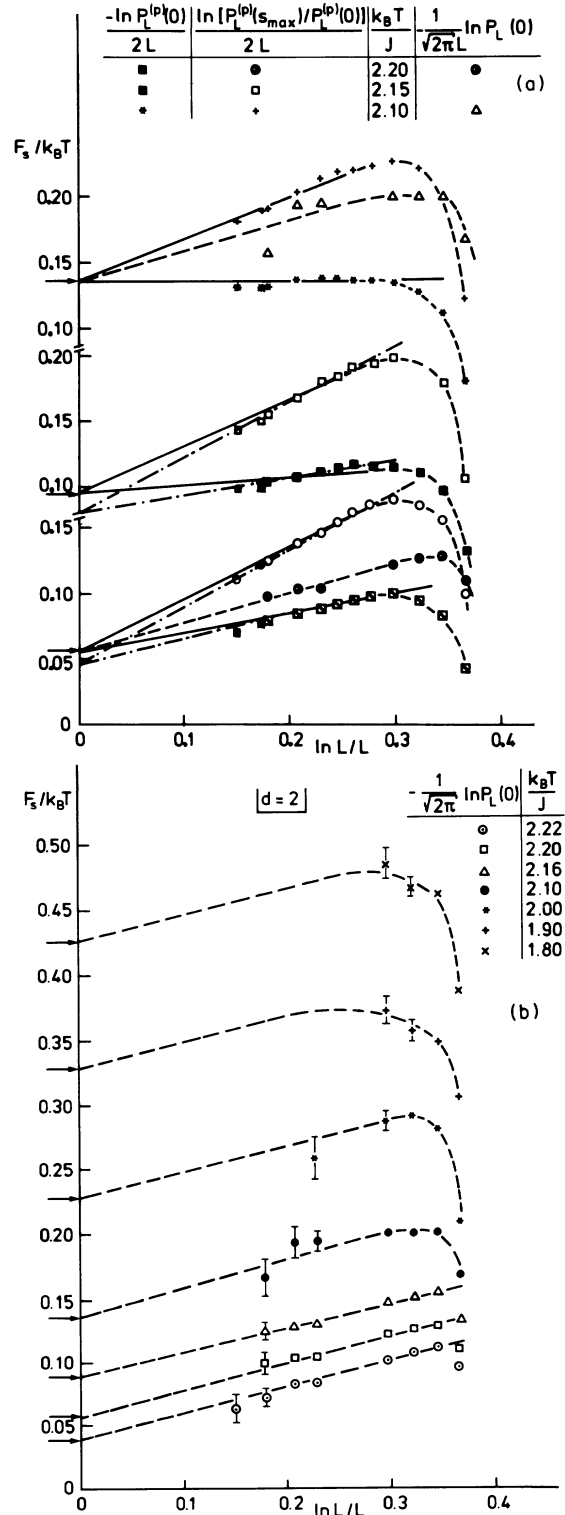


FIG. 5. Extrapolation of $\ln P_L^{(p)}(0)/L$, $\ln[P_L^{(p)}(s_{\max})/P_L^{(p)}(0)]/L$, and $\ln P_L(0)/L$ vs $\ln L/L$ for three temperatures in the critical region. Straight lines indicate various possible extrapolations. (b) $\ln P_L(0)/L$ plotted vs $\ln L/L$. Arrows indicate Eq. (10).

that the exponent x in Eq. (4) is independent of temperature, and thus the slope of the straight lines in Fig. 5(b) was also chosen independent of temperature. Thus also the data on the subsystem block distribution may be consistent with Eq. (10)—although the results for $k_B T/J = 1.8, 1.9,$ and 2.0 for the available values of L clearly lie outside the asymptotic regime where a formula such as Eq. (4) holds, and hence the interpretation given in Fig. 5(b) is only a tentative one. In summary, then, it can be said that clearly the blocks with periodic boundary conditions yield more reliable data on F_s than the subsystem blocks.

IV. THREE-DIMENSIONAL ISING MODEL

Simple cubic Ising lattices with nearest-neighbor exchange and periodic boundary conditions have been studied to obtain $P_L^{(p)}(s=0)$, choosing linear dimensions between $L=2$ and $L=12$ (Fig. 6). In addition, a system of linear dimension $N=24$ was simulated to obtain $P_L(s=0)$ for subsystem blocks, but again we found that the latter data are hard to analyze.

Plotting $\ln P_L^{(p)}(s=0)/L^2$ as well as $\ln[P_L^{(p)}(s_{\max})/P_L^{(p)}(0)]$ vs the variable $1/L^2$ a rather distinct curvature was encountered, while a plot vs the variable $\ln L/L^2$ was closer to linearity (Fig. 7). Within some uncertainty as indicated by the arrows with the error bars, $F_s/k_B T$ can be estimated reliably.

Again one might infer from Eq. (6) that the slopes of this extrapolation shown in Fig. 7 should be independent of temperature, having values $x/2$ and $x/2-d/4$, respectively. We have not imposed

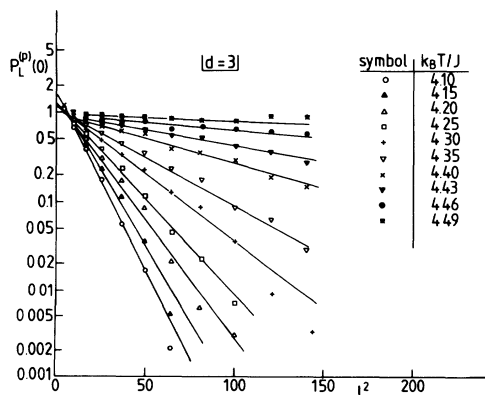


FIG. 6. Semilogarithm plot of $P_L^{(p)}(0)$ vs L^2 for the nearest-neighbor three-dimensional simple-cubic Ising model and various temperatures.

this condition in our extrapolation in Fig. 7, as the apparent difference in slope between the apparent straight lines used in Fig. 7 is much less than the theoretical value $d/4$. Thus it is clear that we are not really in the true asymptotic region where Eq. (6) is valid, which is not surprising since the values of L chosen are of the same order of magnitude as the correlation length ζ . Of course, the same difficulty occurs in the two-dimensional case—the extrapolation via the full and dash-dotted lines in Fig. 5(a) indicates the magnitude of the uncertainty about F_s which one expects in a case where the exact answer is not known. It is clear that sampling $P_L(s=0)$ for values of L where $L \gg \zeta$ would constitute a substantially larger computational effort; the present data have been obtained with runs of $10^4 - 10^5$ Monte Carlo steps per lattice site.

Figure 8 shows the temperature variation of the surface tension. As in the two-dimensional case, data extracted from the apparent slope of $\ln P_L^{(p)}(0)$ vs L^2 plots are slightly but systematically in error. The data of $\ln P_L(0)$ vs L^2 plots are significantly off, indicating that one is still far from the asymptotic region where a spherical domain dominates

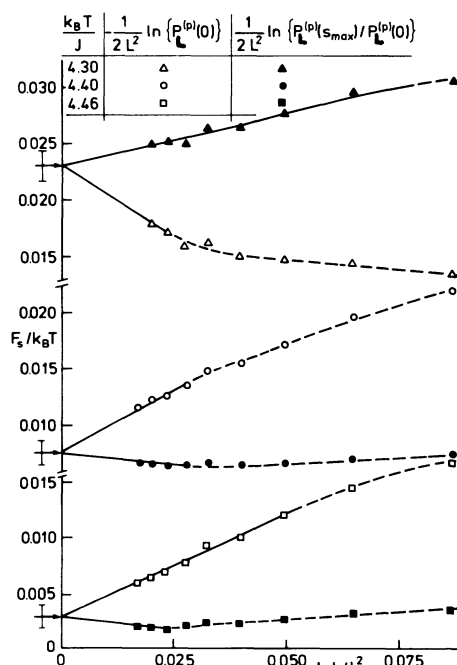


FIG. 7. Extrapolation of $\ln P_L^{(p)}(0)/L^2$ and $\ln[P_L^{(p)}(s_{\max})/P_L^{(p)}(0)]/L$ vs $\ln L/L^2$, for three temperatures close to the critical temperature of the three-dimensional Ising simple-cubic lattice. Arrows indicate our estimates of $F_s/k_B T$.

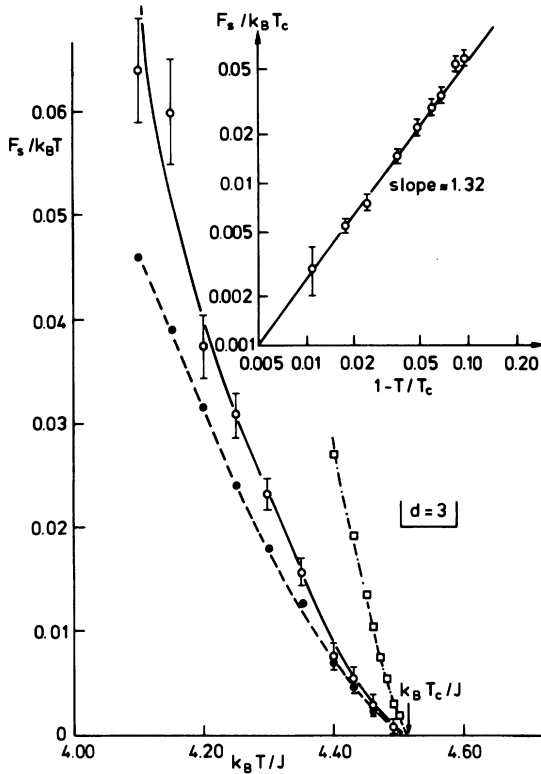


FIG. 8. Surface tension of the simple-cubic nearest-neighbor Ising model plotted vs temperature. Full circles result from the slope of $\ln P_L^{(p)}(0)$ vs L^2 plots (Fig. 6); open circles are extrapolated data (such as obtained in Fig. 7). Squares result from the slope of $\ln P_L(0)$ vs L^2 [for raw data of $P_L(0)$ in three dimensions see Ref. 19]. Insert shows log-log plot of $F_s/k_B T_c$ vs $1-T/T_c$.

the configurations sampled by $P_L(0)$. Thus the apparent surface tension which would follow from $P_L(0)$ is of little practical use, although it also vanishes at the correct critical temperature [$k_B T_c/J \approx 4.51$ (Ref. 25)]. We think, consistent with the experience of the two-dimensional case, that the data obtained from extrapolating $\ln P_L^{(p)}(0)/L^2$ vs $\ln L/L^2$ (Fig. 7) are the most reliable estimates of $F_s/k_B T$ (open circles in Fig. 8). The insert of Fig. 8 shows that these data are in fact consistent with the expected critical behavior: the straight-line fitting the data points of the log-log plot implies

$$F_s/k_B T \cong 1.1 (1-T/T_c)^{1.32}. \quad (11)$$

From hyperscaling relations one expects the surface tension to vary $\propto (1-T/T_c)^{2\nu}$ in three dimensions,¹¹ where ν is the critical exponent of the correlation length. Using the accepted "best value" of ν , which is due to field-theoretical renormalization-group approaches,²⁶ $\nu \approx 0.63$, we conclude

that the exponent of $F_s/k_B T_c$ should be 1.26 rather than 1.32. We attribute this 5% discrepancy to correction terms to the asymptotic critical behavior which are expected in this order of magnitude as we are using data about 10% off T_c . In fact, if one adapts this interpretation, and fits a straight line with the theoretical exponent 1.26 to the data closer than 5% to T_c , one gets an amplitude factor which is only slightly different,

$$F_s/k_B T_c \cong 1.0(1-T/T_c)^{1.26}. \quad (12)$$

As a result, we conclude that the critical amplitude F_s of the surface tension, $F_s/k_B T_c = \hat{F}_s(1-T/T_c)^{(d-1)\nu}$, has the value $\hat{F}_s + 1.05 \pm 0.05$ for $d=3$ [for $d=2$ $\hat{F}_s = 4J/k_B T_c \cong 1.76$ can be seen from Eq. (10)].²⁷

V. UNIVERSAL CRITICAL AMPLITUDE RATIO OF THE SURFACE TENSION

Already from the theory of Widom⁵ it is clear that one can form a certain combination of critical amplitudes of bulk quantities and \hat{F}_s , which should be universal, i.e., the same for all systems belonging to the same universality class. Since three-dimensional liquid-gas critical phenomena, as well as binary critical mixtures, are believed to belong to the same static universality class as the Ising model, it makes sense to compute this universal amplitude ratio for the latter, using the above first estimate of \hat{F}_s .

Defining amplitudes B , C^- , and ξ^- for the critical behavior of the Ising-model order parameter, susceptibility, and correlation length below T_c ,

$$\begin{aligned} \langle S \rangle &= B(1-T/T_c)^\beta, \\ k_B T \chi &= C^-(1-T/T_c)^{-\gamma}, \\ \xi/a &\equiv f_1^-(1-T/T_c)^{-\nu}, \end{aligned} \quad (13)$$

where a is the lattice spacing, β , γ , ν being the critical exponents in usual notation,¹¹ the Fisk-Widom universal amplitude ratio c is expressed as^{5,28}

$$\beta^2 c = \frac{c^- \hat{F}_s}{4B^2 f_1^-}. \quad (14)$$

Using the estimates of c^- and f_1^- due to Tarko and Fisher,²⁹ $C^- \approx 0.209$, $f_1^- \approx 0.244$, and $B \approx 1.569$,²⁵ we obtain, with the estimate of \hat{F}_s as given above, $\beta^2 c \approx 0.092 \pm 0.05$. Here we assume that the error of the amplitudes B , C^- , and f_1^-

can be neglected in comparison with the error of \hat{F}_s . Using the exact two-dimensional results $B \cong 1.2224$,³⁰ $C^- \cong 0.025537$,³¹ $f_1^- \cong 0.176$ (Ref. 29) yields $\beta^2 c \cong 0.0428$. Table I shows that the present estimate for $\beta^2 c$ is in much better agreement with experimental data on SF₆,³² CO₂,³²⁻³⁴ and Xe (Ref. 35) than the value of classical³ or Fisk-Widom⁵ theories or first-order ϵ expansion.¹⁰ Clearly, the latter underestimates the decrease of $\beta^2 c$ with decreasing dimensionality, which is evident from the small value of $\beta^2 c$ in two dimensions. Since the exponent β itself is rather drastically dependent on dimensionality, this observation suggests a study of the d dependence of c itself rather than $\beta^2 c$ as done previously.¹⁰ Figure 9 shows that the first-order ϵ expansion of c rather than $\beta^2 c$ is nearly in agreement with our value (and the experimental data)—it now underestimates the two-dimensional value ($c \approx 2.72$) rather than overestimating it. Of course, one should not use first-order $4-d$ expansion for any dimensionality far below $d=4$.

The critical behavior of the surface tension clearly is also relevant for a description of nucleation phenomena in the critical region.³⁶⁻³⁸ There it is a different combination of critical amplitudes which enters. This is seen by considering the energy barrier ΔF for the formation of a liquid droplet (of radius R) in a supersaturated gas (of density $\langle \rho_- \rangle + \delta\rho$, or associate chemical potential difference $\delta\mu$):

$$\Delta F = -\frac{4\pi R^3}{3} \Delta\rho \delta\mu + 4\pi R^2 F_s, \quad (15)$$

$$(\Delta\rho = \langle \rho_+ \rangle - \langle \rho_- \rangle).$$

From the condition $\partial(\Delta F)/\partial R|_{R^*} = 0$ one finds the critical radius $R^* = 2F_s/(\Delta\rho\delta\mu)$ and hence $\Delta F^* = (16\pi/3)F_s^3/(\Delta\rho\delta\mu)^2$; eliminating then $\delta\mu$ in

favor of the relative density change $\delta\rho/\Delta\rho = (\partial\rho/\partial\mu)_T \delta\mu/\Delta\rho$ one finds

$$\frac{\Delta F^*}{k_B T_c} = \frac{16\pi}{3} \frac{F_s^3 (\partial\rho/\partial\mu)_T^2}{k_B T_c (\Delta\rho)^4 (\delta\rho/\Delta\rho)^2} = \frac{x_0^2}{x^2}, \quad (16)$$

where following the notation of Langer and Schwartz³⁸ we have defined $x = (2/\beta)(\delta\rho/\Delta\rho)$. The (universal) constant x_0^2 then is

$$x_0^2 = \frac{64\pi}{3\beta^2} \frac{F_s^3 (\partial\rho/\partial\mu)_T^2}{k_B T_c (\Delta\rho)^4} = \frac{16\pi}{3\beta^2} \frac{\hat{F}_s^3 C_-^2}{B^4}. \quad (17)$$

Again the result of the present work, $x_0 \approx 1.14 \pm 0.10$, is in reasonable agreement with experimental data for CO₂,³⁴ where³⁸ $x_0 \approx 1.24 \pm 0.10$, and the binary mixture C₇H₁₄-C₇F₁₄,³⁹ where³⁸ $x_0 = 1.30 \pm 0.10$.

Another universal relation between the surface tension and the specific heat C_T ,

$$C_T/k_B = (A^-/\alpha)(1-T/T_c)^{-\alpha},$$

was proposed by Stauffer *et al.*,⁴⁰ considering the quantity

$$Y \equiv \hat{F}_s / (A^-)^{(d-1)/d}. \quad (18)$$

Since the series expansions for the specific heat of the three-dimensional Ising model can be represented near T_c by²⁵ $C_T/k_B \approx 0.20(1-T/T_c)^{-1/8}$, we find from Eq. (18) that $Y \approx 12.3$. On the other hand, experimental data for Xe (Ref. 35) have yielded⁴⁰ $Y = 6.2 \pm 0.6$ and for CO₂ (Ref. 40) $Y = 6.4 \pm 0.4$. For $d=2$, the exact answer is⁴⁰ $Y = \sqrt{2\pi} \cong 2.51$. We feel that the discrepancy between the present estimate and the experimental results (as analyzed in Ref. 40) may reflect the difficulty in precisely estimating the asymptotic behavior of the specific heat, which is largely influenced both by singular correction terms and by regular

TABLE I. The universal constant $\beta^2 c$ of the surface tension. Experimental values are as quoted in Ref. 10.

Classical theory (Ref. 3)		$\frac{1}{6}$
Fisk and Widom (Ref. 5)		0.142
First-order ϵ expansion (Ref. 10)		0.149
Present work		0.092 ± 0.005
	SF ₆ (Ref. 32)	0.093 ± 0.011
		0.110 (Refs. 32 and 33)
Experimental values	CO ₂	0.123 (Ref. 34)
		0.146 (Ref. 34)
	Xe (Ref. 35)	0.100 ± 0.012

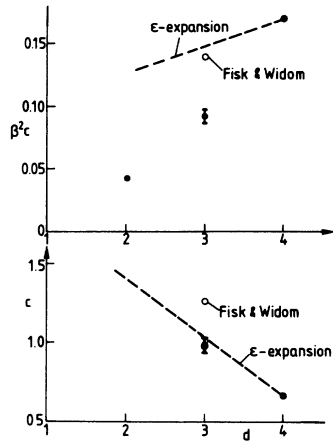


FIG. 9. Universal constants $\beta^2 c$ (upper part) and c (lower part) plotted vs dimensionality. Full circles are the present results, broken line in the upper part is the result of Ref. 10, and open circle is due to Ref. 5. Note that $\beta \approx 0.32$ for $d=3$ (Ref. 26) and $\beta = \frac{1}{8}$ for $d=2$ (Ref. 30).

background terms. This point certainly deserves further study.

VI. CONCLUSIONS

In this paper we have introduced a new method for calculating the interface free energy F_s between coexisting phases, considering the distribution $P_L^{(p)}(\rho)$ of the order parameter ρ distinguishing the phases in finite systems of linear dimension L , using periodic boundary conditions. It is implied that the asymptotic behavior of $P_L^{(p)}(\rho_{\min})$ for large L is an exponential decay, the decay rate being given by $2F_s L^{d-1}/k_B T$. This definition of the interface free energy does not suffer from any conceptual difficulties associated with the existence of a well-localized interface profile.

It has been further suggested that this concept yields a useful method to estimate F_s numerically from computer simulations, for cases where $F_s/k_B T \ll 1$. This in general is expected to be true in the vicinity of the critical temperature (where the order parameter $\Delta\rho = \langle\rho_+\rangle - \langle\rho_-\rangle$ vanishes). In fact, use of this method for the two-dimensional Ising model, where F_s is known exactly, yielded results reasonably consistent with the exact solution. At the same time, the distribution $P_L(\rho_{\min})$ in subsystem blocks, which, in principle, also would be suitable for estimating F_s , in practice

is not useful for this purpose, for the range of linear dimensions L which is conveniently accessible in practice.

We have also applied the same method for the three-dimensional Ising system, and found the surface tension to be consistent with a critical behavior $F_s/k_B T_c \approx 1.03(1 - T/T_c)^{2\nu}$, which constitutes the first estimate of its critical amplitude. Together with information on other critical properties of the Ising model, we have estimated the universal constant $\beta^2 c$ of the surface tension introduced by Fisk and Widom. Our value for this constant is much closer to most experimental data than the estimate of these authors or the result of first-order renormalization-group expansions. Also the universal amplitude entering the description of nucleation theory near the critical point is calculated and reasonably close to estimates based on experimental data. However, an unexplained discrepancy remains concerning the universal amplitude ratio of Stauffer *et al.*

The present method could be applied to more complicated models in a similar fashion. In a simulation of a Lennard-Jones fluid, one would use the grand-canonical ensemble and study the density distribution function. The approach is somewhat more difficult, as it is nontrivial to adjust the system at the chemical potential $\mu_{\text{coex}}(T)$, which is not known *a priori*. [If one uses a chemical potential slightly off the value at the coexistence curve, the distribution function $P_L^{(p)}(\rho)$ should asymptotically tend towards the density distribution of a one-phase state, exhibiting one peak only rather than two peaks.] Still the method could be useful as one simultaneously can estimate both F_s and $\mu_{\text{coex}}(T)$. As regards critical properties of fluids or binary mixtures, they belong to the same universality class as the Ising system studied here, and hence their universal amplitude ratios should be the same as those obtained here.

ACKNOWLEDGMENTS

Thanks are due to R. K. P. Zia for discussions. The author is particularly grateful to W. Oed for his help with the use of the FPS AP 190L array processor on which part of the computations were performed.

- ¹Following the standard use of this term, surface tension is used to denote the interface free energy per unit interface area. We are not concerned here with other types of boundaries of a system, to which one also may associate a surface free energy, such as "walls," etc.; see, e.g., K. Binder and P. C. Hohenberg, *Phys. Rev. B* **6**, 3461 (1972) for a discussion of other such surfaces in the context of Ising models.
- ²J. D. van der Waals, *Z. Phys. Chem.* **13**, 657 (1894).
- ³J. W. Cahn and J. E. Hilliard, *J. Chem. Phys.* **28**, 258 (1958).
- ⁴O. K. Rice, *J. Phys. Chem.* **64**, 976 (1960).
- ⁵S. Fisk and B. Widom, *J. Chem. Phys.* **50**, 3219 (1969); see also B. Widom, *ibid.* **43**, 3892 (1965).
- ⁶B. U. Felderhof, *Physica* **48**, 541 (1970).
- ⁷D. G. Triezenberg and R. W. Zwanzig, *Phys. Rev. Lett.* **28**, 1183 (1972).
- ⁸F. F. Abraham, *Phys. Rep.* **53**, 93 (1979), and references therein.
- ⁹K. W. Sarkies and N. E. Frankel, *Phys. Rev. A* **11**, 1724 (1975).
- ¹⁰T. Ohta and K. Kawasaki, *Prog. Theor. Phys.* **58**, 467 (1977); see also J. Rudnick and D. Jasnow, *Phys. Rev. B* **17**, 1351 (1978).
- ¹¹B. Widom, in *Phase Transitions and Critical Phenomena*, edited by C. Domb and M. S. Green (Academic, New York, 1972), Vol. II, p. 79.
- ¹²F. P. Buff, R. A. Lovett, and F. H. Stillinger, Jr., *Phys. Rev. Lett.* **15**, 621 (1965).
- ¹³J. Zittartz, *Phys. Rev.* **154**, 529 (1967).
- ¹⁴L. Onsager, *Phys. Rev.* **65**, 117 (1944); see also D. Abraham and P. Reed, *J. Phys. A* **10**, L121 (1977).
- ¹⁵Effects of capillary waves would be included if one could calculate the interface free energy from the renormalization-group expansion around the lower critical dimensionality $d_l = 1$. So far this $1 + \epsilon$ expansion has been applied to bulk critical properties only; see D. J. Wallace and R. K. P. Zia, *Phys. Rev. Lett.* **43**, 808 (1979).
- ¹⁶For a short review, see D. Levesque, J.-J. Weis, and J.-P. Hansen, in *Monte Carlo Methods in Statistical Physics*, edited by K. Binder (Springer, Berlin, 1979), p. 112.
- ¹⁷H. J. Leamy, G. H. Gilmer, K. A. Jackson, and P. Bennema, *Phys. Rev. Lett.* **30**, 601 (1973).
- ¹⁸C. H. Bennett, *J. Comp. Phys.* **22**, 245 (1976); J. Miyazaki, J. A. Barber, and G. M. Pound, *J. Chem. Phys.* **64**, 3364 (1976).
- ¹⁹K. Binder, *Z. Phys. B* **43**, 119 (1981).
- ²⁰In principle, one should also consider contributions from domain configurations with more than two interfaces, as well as all possible domain shapes. For large L , however, the domain shape with minimum interface area nearly exhausts the probability $P_L^{pp}(\rho_{\min})$. This shape is obtained for one domain with two flat interfaces, in the case of periodic boundary conditions. Neither position nor orientation of these two interfaces inside the cell is fixed. The condition $\rho = \rho_{\min}$ requires only that the volumes of the two domains with $\rho = \rho_+$ and $\rho = \rho_-$ are equal.
- ²¹See also L. S. Schulman, *J. Phys. A* **13**, 237 (1980).
- ²²C. Rottman and M. Wortis (unpublished).
- ²³J. E. Avron and R. K. P. Zia (unpublished); J. E. Avron, H. van Beijeren, L. S. Schulman, and R. K. P. Zia (unpublished).
- ²⁴Unintentionally it is not the order-parameter distribution $P_L(\rho)$ which was studied numerically but a slightly different distribution $P'_L(\rho)$. In terms of the M states $\{\rho_i\}$ generated in the Markov process these distributions can be expressed as $P_L(\rho) \propto (1/M) \sum_{i=1}^M \delta(\rho_i - \rho)$ and $P'_L(\rho) \propto (1/M) \sum_{i=1}^M \delta(\rho_i - \rho) / W(\rho_i)$, where $W(\rho_i)$ is the transition probability (for a single spinflip) in state ρ_i . Since $W(\rho)$ is a very smooth function of its argument, the distributions $P_L(\rho)$ and $P'_L(\rho)$ are qualitatively similar, and tend towards the same distribution for large L . Both distributions should be equally well suited for an analysis as carried through in this paper. In the following the distinction between $P_L(\rho)$ and $P'_L(\rho)$ is disregarded.
- ²⁵C. Domb, in *Phase Transitions and Critical Phenomena*, Vol. 3, edited by C. Domb and M. S. Green (Academic, New York, 1974) p. 357.
- ²⁶J. C. Le Guillou and J. Zinn-Justin, *Phys. Rev. B* **21**, 3976 (1980).
- ²⁷Taking the derivative of $F_s/k_B T$ as given by Eq. (11) or Eq. (12) with respect to $1/k_B T$, we obtain the interface internal energy E_s/J . The result agrees with the estimates of Ref. 17, within the rather large error bars of the latter calculation.
- ²⁸From Eq. (21) of Ref. 5, in our notation, $F_s/k_B T = c\beta^2(\xi/\chi_\rho) (\langle \rho_+ \rangle - \langle \rho_- \rangle)^2$ we obtain Eq. (14) using the Ising magnet-lattice-gas transcription, where $\rho = (1 + \langle s \rangle)/2$, the magnetic field H being related to the chemical potential μ by $H = (\mu - \mu_{\text{coex}})/2$, $\chi_\rho = (\partial \rho / \partial \mu)_T = (\partial M / \partial H)_T / 4$.
- ²⁹H. B. Tarko and M. E. Fisher, *Phys. Rev. B* **11**, 1217 (1975).
- ³⁰C. N. Yang, *Phys. Rev.* **85**, 808 (1952).
- ³¹T. T. Wu, B. M. McCoy, C. A. Tracy, and E. Barouch, *Phys. Rev. B* **13**, 316 (1976).
- ³²E. S. Wu and W. W. Webb, *Phys. Rev. A* **8**, 2065 (1973); **8**, 2077 (1973).
- ³³M. A. Bouchiat and J. Meunier, *Phys. Rev. Lett.* **23**, 752 (1969).
- ³⁴J. C. Herpin and J. Meunier, *J. Phys. (Paris)* **35**, 847 (1974).
- ³⁵J. Zollweg, G. Hawkins, and G. B. Benedek, *Phys. Rev. Lett.* **27**, 1182 (1971).
- ³⁶K. Binder and D. Stauffer, *Adv. Phys.* **25**, 343 (1976).
- ³⁷K. Binder, *J. Phys. (Paris)* **41**, C4-51 (1980).
- ³⁸J. S. Langer and A. J. Schwartz, *Phys. Rev. A* **21**, 948 (1980).
- ³⁹R. B. Heady and J. W. Cahn, *J. Chem. Phys.* **58**, 896 (1973).
- ⁴⁰D. Stauffer, M. Ferer, and M. Wortis, *Phys. Rev. Lett.* **29**, 345 (1972).